ARTICLE IN PRESS

Soils and Foundations ▮▮▮▮;▮(▮):▮▮▮–▮▮▮

The Japanese Geotechnical Society

Soils and Foundations

www.sciencedirect.com
journal homepage: www.elsevier.com/locate/sandf

# Probabilistic analysis of obliquely loaded strip foundations

Abdul-Hamid Soubra*, Nut Mao[1]

*University of Nantes, Bd. de l'université, BP 152, 44603 Saint-Nazaire Cedex, France*

**Abstract**

This paper presents a probabilistic analysis at the ultimate limit state of a shallow strip footing resting on a ($c$, $\varphi$) soil and subjected to an inclined load. The system response considered in the analysis is the safety factor obtained using the strength-reduction technique. The deterministic model makes use of the kinematic approach of the limit analysis theory. The Polynomial Chaos Expansion (*PCE*) methodology is employed for the probabilistic analysis. The soil shear strength parameters and the footing load components are considered as random variables. A reliability analysis and a global sensitivity analysis are performed. Also, a parametric study showing the effect of the different statistical characteristics of the random variables on the variability of the safety factor is presented and discussed. It is shown that the use of the safety factor (based on the strength-reduction technique) for the system response is of significant interest in the reliability analysis, since it takes into account the simultaneous effect of soil punching and footing sliding and it requires a unique reliability analysis for both failure modes. Furthermore, it allows the rigorous determination of the zones of predominance of soil punching and footing sliding in the interaction diagram for different cases of soil and/or loading uncertainties. Finally, it is shown that the loading configurations located in the zone of the footing sliding predominance exhibit a more significant variability in the safety factor compared to those located in the zone of the soil punching predominance.


*Keywords:* Shallow foundation; Reliability; Polynomial Chaos Expansion method; Limit analysis; Safety factor

## 1. Introduction

Traditionally, stability analyses of shallow foundations have been based on deterministic approaches (Kusakabe et al., 1981; Michalowski, 1997; De Buhan and Garnier, 1998; Soubra, 1999; Kusakabe and Kobayashi, 2010). In these approaches, the uncertainties of the input parameters are taken into account through the use of a global safety factor. Reliability-based analyses are more rational, however, since they allow for consideration of the inherent uncertainty of each uncertain parameter. Nowadays, this is possible because of improvements in our knowledge of the statistical properties of soil (Phoon and Kulhawy, 1999).

Previous investigations of reliability-based analyses of foundations focused on shallow strip footings subjected to a central vertical load (Bauer and Pula, 2000; Cherubini, 2000; Griffiths and Fenton, 2001; Griffiths et al., 2002; Fenton and Griffiths, 2002, 2003; Popescu et al., 2005; Przewlocki, 2005; Sivakumar Babu and Srivastava, 2007; Youssef Abdel Massih et al., 2008; Youssef Abdel Massih and Soubra, 2008). In this paper, a reliability analysis at the ultimate limit state (ULS) of a shallow strip footing, subjected to inclined loading, is presented.

Contrary to the case of vertical loading, where only soil punching may occur, both soil punching as well as footing sliding are present in the case of inclined loading, and

*Corresponding author. Tel.: +33 240 905 106; fax: +33 240 905 109.
*E-mail addresses:* Abed.Soubra@univ-nantes.fr (A.-H. Soubra), mao_nut@yahoo.com (N. Mao).
[1]Tel.: +33 240 905 108; fax: +33 240 905 109.



Peer review under responsibility of The Japanese Geotechnical Society
http://dx.doi.org/10.1016/j.sandf.2012.05.010

Production and hosting by Elsevier

**Nomenclature**

| | |
|---|---|
| $\alpha_i$, $\beta_i$ | angular parameters of the triangular rigid block $i$ |
| $\alpha$ | load inclination |
| $\beta_{HL}$ | Hasofer–Lind reliability index |
| $\gamma$ | soil unit weight |
| $\mu$ | mean value |
| $\mu_H$ | mean value of the horizontal load component |
| $\mu_V$ | mean value of the vertical load component |
| $\mu_{Vopt}$ | optimal mean value of the vertical load component |
| $\xi$ | vector composed of four standard normal variables |
| $\xi_1$, $\xi_2$, $\xi_3$, $\xi_4$ | four standard normal variables that represent c, $\varphi$, $V$ and $H$, respectively |
| $\rho$ | coefficient of correlation |
| $\sigma$ | standard deviation |
| $\sigma_H^N$ | equivalent normal standard deviation of the horizontal load component |
| $\sigma_V^N$ | equivalent normal standard deviation of the vertical load component |
| $\psi_\beta$ | multidimensional Hermite polynomial |
| $\varphi$ | soil friction angle |
| $\varphi_d$ | developed soil friction angle |
| $a_\beta$ | unknown coefficients of the *PCE* |
| $A$ | information matrix |
| $B_0$ | width of the strip footing |
| $c$ | soil cohesion |
| $c_d$ | developed soil cohesion |
| COV | coefficient of variation |
| $\dot{D}$ | energy dissipation |
| $d_i$, $l_i$ | velocity discontinuity lines of the triangular rigid block $i$ |
| $F_{punching}$ | punching safety factor |
| $F_s$ | safety factor obtained using the strength reduction technique |
| $F_{sliding}$ | sliding safety factor |
| $G$ | performance function |
| GSA | global sensitivity analysis |
| $H_u$ | ultimate horizontal load component |
| $H$ | applied horizontal load component |
| $k$ | number of triangular rigid blocks |
| $M$ | number of input random variables |
| MCS | Monte Carlo Simulation |
| $N$ | number of the available sampling points |
| $p$ | order of the *PCE* |
| $P$ | number of unknown coefficients $a_\beta$ |
| *PCE* | Polynomial Chaos Expansion |
| *PDF* | probability density function |
| $P_f$ | failure probability |
| $R^2$ | coefficient of determination |
| SU | Sobol index |
| ULS | ultimate limit state |
| $V$ | applied vertical load component |
| $V_u$ | ultimate vertical load component |
| $v_i$ | velocity of block $i$ |
| $v_{i,i+1}$ | inter-block velocity between blocks $i$ and $i+1$ |
| $\dot{W}$ | rate of work of external forces |
| $Y$ | vector of model response values |

therefore, should be considered in the analysis. The soil shear strength parameters ($c$, $\varphi$) and the applied load components (vertical $V$ and horizontal $H$) are considered as uncertain parameters. These four uncertain parameters are modeled herein by random variables [i.e., they are characterized by their probability density functions (*PDF*s)]. The deterministic model is analytical and is based on the kinematic approach of the limit analysis theory. The system response considered in the analysis is the safety factor obtained using the strength-reduction technique. The use of such a safety factor allows for the simultaneous consideration of the two failure modes (soil punching and footing sliding) using a single simulation. This is particularly useful in reliability-based analyses, since a unique reliability analysis is required for both failure modes.

As for the probabilistic analysis, the classical Monte Carlo Simulation (*MCS*) methodology is generally used to compute either the *PDF* of the system response or the failure probability $P_f$. In spite of being a rigorous and robust methodology, *MCS* requires a great number of calls for the deterministic model (about 1,000,000 samples for a failure probability of $10^{-5}$). In the present paper, a more efficient method based on the Polynomial Chaos Expansion (*PCE*) is used (Isukapalli et al., 1998; Huang et al., 2009; Mollon et al., 2011; Houmadi et al., 2012; Mao et al., 2012). This method requires a much smaller number of calls for the deterministic model.

The *PCE* methodology allows the replacement of the deterministic model, for which the input uncertain parameters are modeled by random variables, by an approximate simple analytical equation. In the present paper, the analytical equation provided by the *PCE* methodology allows the determination of the safety factor as a function of four standard normal variables that represent the four input uncertain parameters, $c$, $\varphi$, $V$ and $H$. Thus, the probabilistic analysis can be easily performed when using the Monte Carlo Simulation. This is because the safety factor can be computed at a negligible time cost when using the simple analytical equation.

The aim of the paper is threefold. Firstly, a global sensitivity analysis is performed. The aim of this analysis is to provide the contribution of each input random variable ($c$, $\varphi$, $V$ and $H$) in the variability of the safety factor. Secondly, the zones of the interaction diagram, corresponding to the predominance of the footing sliding or the soil punching, are determined for different cases of soil and/or loading uncertainties. Finally, a parametric study showing the effect of the different statistical characteristics of the random variables (type of *PDF*, coefficient of variation *COV* and coefficient of correlation $\rho$) on the *PDF* of the safety factor is presented and discussed. It should be mentioned here that the present work has been undertaken as part of a broader objective, namely, to perform a probabilistic analysis of offshore foundations (such as spudcans, bucket foundations, suction caissons, etc.) subjected to eccentric and inclined loading and taking into account the soil and the loading uncertainties.

The aim of the next sections is to present (i) the deterministic model used for the computation of the safety factor of the soil-footing system, (ii) the *PCE* methodology employed for the probabilistic analysis and (iii) the probabilistic results. The paper ends with a conclusion.

## 2. Limit analysis model

In this paper, a non-symmetrical kinematically admissible failure mechanism, based on the upper-bound theorem of the limit analysis, is used for the deterministic model. This mechanism was presented by Soubra (1999) for the computation of the ultimate bearing capacity of strip footings situated in seismic areas by a pseudo-static approach. It is a translational multiblock failure mechanism (Fig. 1a) and is composed of $k$ triangular rigid blocks. This mechanism can be completely described by $2k-1$ angular parameters which are $\alpha_i$ ($i=1, \ldots, k-1$) and $\beta_i$ ($i=1, \ldots, k$). The first wedge ABC of this mechanism is assumed to translate with a velocity $v_1$ inclined at an angle $\varphi$ to velocity discontinuity line AC (Fig. 1b). The foundation is assumed to move with the same velocity as wedge

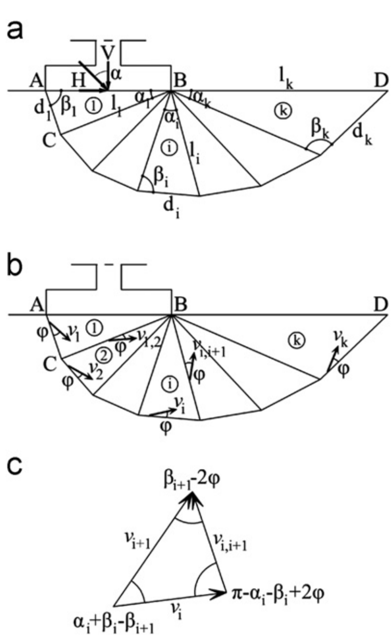


Fig. 1. (a) Translational non-symmetrical multiblock failure mechanism, (b) velocity field, and (c) velocity hodograph.

ABC (i.e., $v_1$). The other velocities $v_i$ of wedge $i$ ($i=2, \ldots, k$) and the inter-wedge velocities $v_{i,i+1}$ ($i=1, \ldots, k-1$) are assumed to be inclined at an angle $\varphi$ to the corresponding velocity discontinuity lines (i.e., $d_i$ or $l_i$) in order to respect the normality condition imposed by the theory of limit analysis. The velocity hodograph is presented in Fig. 1(c).

For this mechanism, the work equation is obtained by equating the total rate of work $\dot{W}$ of the external forces to the total rate of energy dissipation $\dot{D}$ along the lines of velocity discontinuities $d_i$ and $l_i$. For more details on this mechanism, the reader should refer to Soubra (1999).

The response considered in the analysis is not the ultimate bearing capacity, as was the case in Soubra (1999). Indeed, the stability analysis of a strip footing subjected to an inclined load is traditionally performed by computing two individual safety factors, $F_{punching}=V_u/V$ and $F_{sliding}=H_u/H$, against soil punching and footing sliding, respectively, where $V_u$ and $H_u$ are the vertical and the horizontal ultimate loads. These safety factors, which consider only a single mode of failure (punching or sliding), are not very rigorous, since both failure modes (footing sliding and soil punching) simultaneously exist whatever the values for the footing load components ($V$, $H$) may be. A more rigorous method, based on the strength-reduction technique, is proposed herein for the computation of a unique rigorous safety level that simultaneously takes into account the two modes of failure. In this method, the soil shear strength parameters ($c$ and $\varphi$) that appear in the work equation are replaced by $c_d$ and $\varphi_d$, where $c_d$ and $\varphi_d$ are the developed soil shear strength parameters due to the applied footing loads. They are given by

$$c_d = \frac{c}{F_s} \tag{1}$$

$$\varphi_d = ar\tan\left(\frac{\tan\varphi}{F_s}\right) \tag{2}$$

Critical safety factor $F_s$ is obtained by minimization with respect to the mechanism's geometrical parameters. The obtained $F_s$ is the safety factor of the soil-foundation system subjected to the loads ($V$, $H$). As may be seen, the present definition of safety allows for the simultaneous consideration of the two failure modes (footing sliding and soil punching) using a single simulation. Thus, it is particularly useful in probabilistic analyses, since there is no need to perform two separate probabilistic analyses to determine the system failure probability.

## 3. Probabilistic analysis by the Polynomial Chaos Expansion (*PCE*) methodology

In the Polynomial Chaos Expansion methodology, the system response is approximated by a simple analytical formula called *PCE*. Thus, the *PDF* of the system response can be easily obtained by generating a large number of simulations using this *PCE* (not the original deterministic model). In the present paper, the system response is safety factor $F_s$. It was written in the framework of the *PCE* methodology as a function of four standard normal variables, $\xi_1$, $\xi_2$, $\xi_3$ and $\xi_4$, which represent the four input uncertain parameters, $c$, $\varphi$, $V$ and $H$. Thus, the *PDF* of the safety factor can be easily obtained with no time cost by generating a large number of realizations of the vector ($\xi_1$, $\xi_2$, $\xi_3$ and $\xi_4$) and by computing the corresponding system response values using the obtained *PCE*. The *PCE* of the safety factor has the following form (see Huang et al., 2009; Mollon et al., 2011; Houmadi et al., 2012 and Mao et al., 2012 among others):

$$F_s \cong \sum_{\beta=0}^{P-1} a_\beta \Psi_\beta(\xi) \tag{3}$$

where $\xi$ is a vector composed of four standard normal variables, $a_\beta$ are unknown coefficients to be computed and $\Psi_\beta(\xi)$ are multidimensional Hermite polynomials. They are given in the Appendix. For a *PCE* of degree $p$, one should retain only the multidimensional polynomials of a degree less than or equal to the *PCE* order $p$. This leads to a number $P$ of unknown coefficients given by

$$P = \frac{(M+p)!}{M!p!} \tag{4}$$

where $M$ is the number of random variables. The coefficients $a_\beta$ in Eq. (3) may be efficiently computed using a regression approach. This means that the *PCE* is simply obtained by fitting Eq. (3) with the values of the safety factor computed at different sampling points in the standard space of the random variables. These sampling points are determined as follows: the roots of the one-dimensional Hermite polynomial (of one degree higher than the *PCE* order $p$) are computed for each random variable (Isukapalli et al., 1998 and Huang et al., 2009 among others). The sampling points are the results of all possible combinations of these roots for the different random variables. Thus, the number $N$ of the available sampling points depends on the number $M$ of the random variables and the *PCE* order $p$ as follows:

$$N = (p+1)^M \tag{5}$$

It should be mentioned here that in order to perform the deterministic calculations, the independent standard normal random variables of a given sampling point must be transformed to the physical correlated non-normal space (if the physical variables are correlated and non-normal). The reader may find a detailed description on these transformations in Mollon et al. (2011).

As may be seen from Eq. (5), the number of available sampling points dramatically increases as $p$ or $M$ increases. This number is always higher than the number $P$ of the unknown coefficients (given by Eq. (4)) when $M \geq 2$. This leads to a linear system of equations whose number of equations $N$ is greater than the number of unknowns $P$. Based on the regression approach, the vector of the unknown coefficients can be solved by

$$a_\beta = (\Omega^T \Omega)^{-1} \Omega^T Y \tag{6}$$

where $Y = \{Y^1, \ldots, Y^N\}$ is the vector of the model response values (i.e., $F_s$ values in this analysis) computed via the deterministic model for the $N$ sampling points and $\Omega$ is the matrix of dimensions $N \times P$. It is given by

$$\Omega = \begin{bmatrix} \psi_0^1(\xi) & \psi_1^1(\xi) & \cdots & \psi_{P-1}^1(\xi) \\ \psi_0^2(\xi) & \psi_1^2(\xi) & \cdots & \psi_{P-1}^2(\xi) \\ \vdots & \vdots & \ddots & \vdots \\ \psi_0^N(\xi) & \psi_1^N(\xi) & \cdots & \psi_{P-1}^N(\xi) \end{bmatrix} \tag{7}$$

Several attempts have been made in the literature to select the most efficient number of sampling points among the $N$ available ones to reduce the number of calls for the deterministic model (Isukapalli et al., 1998; Berveiller et al., 2006; Sudret, 2008). The approach proposed by Sudret (2008) is a rational methodology. It is based on the invertibility of the information matrix $A = \Omega^T \Omega$ and will be used in this paper. Finally, it should be noted that the quality of the output approximation, *via* a *PCE*, closely depends on the *PCE* order $p$. To ensure a good fit between the *PCE* and the true deterministic model (i.e., to obtain the optimal *PCE* order), the classical coefficient of determination $R^2$ is used. The value $R^2 = 1$ indicates a perfect fit of the true model response, whereas $R^2 = 0$ indicates a nonlinear relationship between the true model and the *PCE* model.

Once the approximation of the safety factor, *via* a *PCE*, has been obtained, this *PCE* can be employed for the probabilistic analyses. The *PDF* of the safety factor and the corresponding statistical moments (i.e., mean $\mu$ and standard deviation $\sigma$) can be easily estimated. This can be done by simulating a large number of realizations of the vector ($\xi_1$, $\xi_2$, $\xi_3$ and $\xi_4$), using the Monte Carlo Simulation technique, and by computing the safety factor, corresponding to each realization, using the obtained *PCE*. Another important outcome of the *PCE* is that its coefficients can be used to perform a global sensitivity analysis (*GSA*) based on Sobol indices. The *GSA* is generally based on the decomposition of the response variance as a sum of the contributions of the different random variables. The sum of all Sobol indices should be equal to 1. In this paper, the Sobol indices give the contribution of each random variable ($c$, $\varphi$, $V$ or $H$) in the variability of the safety factor. Thus, it is possible to determine the random variables that mostly or moderately contribute to the variability of the safety factor and those that do not significantly contribute to this variability. For more details on the computation of the Sobol indices, using the values of the *PCE* coefficients, the reader may refer to Mollon et al. (2011), among others.

## 4. Numerical results

A strip footing of width $B_0 = 2$ m, placed on a soil mass with a unit weight $\gamma = 18$ kN/m$^3$, is considered in the

Table 1
Illustrative values of the statistical characteristics of the input random variables ($c$, $\varphi$, $V$, $H$).

| Variables | Mean | COV (%) | Probability density function | | Coefficient of correlation |
|---|---|---|---|---|---|
| | | | Case of normal variables | Case of non-normal variables | |
| $c$ (kPa) | 20 | 20 | Normal | Log-normal | $\rho(c, \varphi)=0$ |
| $\varphi$ (deg) | 30 | 10 | Normal | Beta | |
| $V$ (kN/m) | 250* <br> 1000** | 10 | Normal | Log-normal | |
| $H$ (kN/m) | 100*** | 30 | Normal | Log-normal | |

*For point K in Fig. 2.
**For point L in Fig. 2.
***For points K and L in Fig. 2.

analysis. As mentioned before, the soil shear strength parameters ($c$ and $\varphi$) and the applied footing loads ($V$ and $H$) are considered as random variables. Thus, they are characterized by their types of *PDF*s (Gaussian, log-normal, beta, etc.), their mean values $\mu_i$ and their standard deviation values $\sigma_i$ (or their coefficient of variation values $COV_i$ defined as the ratio between $\sigma_i$ and $\mu_i$), where $i=c, \varphi$, $V$ and $H$. In order to incorporate the possible dependence between soil shear strength parameters $c$ and $\varphi$, a correlation coefficient was considered herein. In this paper, the illustrative values used for the coefficient of correlation and the statistical moments of the different input random variables are given in Table 1. However, other values for these parameters were considered within the framework of the parametric study. Notice that the high value of 30% is proposed for the coefficient of variation of the horizontal load component $H$ to represent the large uncertainties due to the wind and/or the wave loading. This value is to be compared to the value of 10% affected to the coefficient of variation of footing vertical load component $V$. This is because $V$ represents the structure weight for which the variability is small. On the other hand, it has been found by several authors (Phoon and Kulhawy, 1999 among others) that the soil friction angle has a small variability [$COV(\varphi)=10\%$]; however, the variability of the soil cohesion may vary in the range 10–40% and may attain 80% in some cases. In this paper, $COV(c)$ was assumed to be equal to 20%. For the type of probability density function for the random variables, two cases were studied. In the first case, referred to as normal variables, $c$, $\varphi$, $V$ and $H$ were considered as normal variables. In the second case, referred to as non-normal variables, $c$, $V$ and $H$ were assumed to be log-normally distributed, while $\varphi$ was assumed to be bounded and a beta distribution was used. Notice that the log-normal distribution is more desirable than the normal distribution, since it guarantees that the random variable is always positive. This type of distribution has been advocated by several investigators (Huang et al., 2010 among others). Notice also that the assumption of the beta distribution for $\varphi$ was proposed by Fenton and Griffiths (2003).

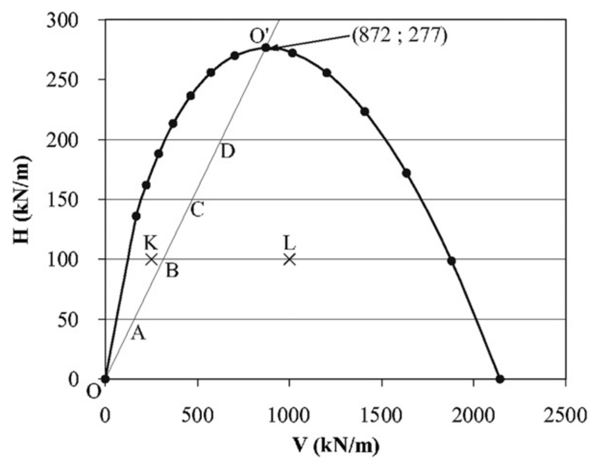


Fig. 2. Interaction diagram ($V$, $H$) for an obliquely loaded footing.

The deterministic model used in this paper is based on the failure mechanism presented in a previous section. An interaction diagram is provided in Fig. 2 using the mean values of soil shear strength parameters $c$ and $\varphi$. Each point ($V_u$, $H_u$) of this diagram corresponds to a given load inclination $\alpha$. The value of $V_u$ is determined by minimization with respect to the mechanism's geometrical parameters; the corresponding $H_u$ value is given by $H_u=V_u(\tan\alpha)$. The maximum point of this diagram is ($V_u=872$ kN/m, $H_u=277$ kN/m).

The probabilistic numerical results, which will be presented in this section, involve the determination of the optimal *PCE* order, the computation of Sobol indices and the correlation coefficients between the input uncertain parameters ($c$, $\varphi$, $V$ and $H$) and the output ($F_s$). This is followed by the determination of the zones of predominance of the soil punching or the footing sliding in the interaction diagram for different cases of soil and/or loading uncertainties. A reliability analysis of several practical load configurations is then presented and discussed. Finally, a parametric study is conducted in order to examine the effect of the statistical parameters of the input random variables on the variability of the system response (i.e., safety factor).

### 4.1. Optimal PCE order, Sobol indices and correlation between the input uncertain variables and the system output

The optimal order of a *PCE* was determined in this paper as the minimal order that leads to a coefficient of determination $R^2$ greater than a prescribed value (say 0.999). Two load configurations (cf., points K and L in the interaction diagram of Fig. 2) were considered for these computations. The numerical results have shown that for both cases, a fourth order *PCE* is necessary in order to satisfy the prescribed condition for the coefficient of determination. Thus, this *PCE* order will be used in all subsequent probabilistic calculations performed in this paper. Remember here that the *PCE*s were constructed using the regression approach based on the concept of matrix invertibility proposed by Sudret (2008). According to this methodology, the number of sampling points required for a fourth order *PCE* with four random variables is equal to 107 points, which corresponds to a reduction by 82.9% with respect to the total available sampling points (i.e., 625 points).

Table 2 presents the Sobol indices of the different input random variables ($c$, $\varphi$, $V$ and $H$) for points K and L shown in Fig. 2. For point K ($V$=250 kN/m, $H$=100 kN/m), one can see that the Sobol index of horizontal load component $H$ is significant (it involves more than 2/3 of the variability of the safety factor), while that of vertical load component $V$ is negligible. This may be explained by (i) the high variability of $H$ and (ii) the predominance of the sliding mode of failure with respect to the punching mode of failure due to the proximity of point K to the left hand branch of the interaction diagram (cf., Fig. 2). Finally, it should be noted that the two other parameters, $c$ and $\varphi$, have moderate values for their Sobol indices (11.0% and 12.7%, respectively), and thus, they contribute moderately to the variability of the safety factor. On the other hand, for point L ($V$=1000 kN/m, $H$=100 kN/m), friction angle $\varphi$ has the greatest Sobol index (it involves more than 2/3 of the variability of the safety factor). The Sobol index for cohesion $c$ is smaller, but not negligible (about 17%), while those of $V$ and $H$ are three times smaller than that for cohesion $c$. These results may be explained by the fact that point L is far from the sliding zone and that soil punching is most likely predominant. In this case, the parameters that mostly contribute to the variability of the safety factor are the soil friction angle, and to a lesser degree, the soil cohesion. Table 2 also shows the coefficients of correlation between the different input random variables ($c$, $\varphi$, $V$ and $H$) and safety factor $F_s$. One can observe that a high correlation exists between an input random variable and the safety factor when the Sobol index of this variable is significant.

From this study, it can be concluded that the variability of $V$ can be neglected (i.e., $V$ can be considered as a deterministic parameter) and $H$ is the variable that mostly contributes to the variability of the safety factor in the zone of footing sliding predominance. However, in the zone of soil punching predominance, soil shear strength parameters $c$ and $\varphi$ are the parameters that mostly contribute to the variability of the safety factor.

### 4.2. Zones of predominance of soil punching or footing sliding

Fig. 3 presents the factor of safety versus vertical load component $V$ for four different values of horizontal load component $H$ ($H$=50 kN/m, 100 kN/m, 150 kN/m and 200 kN/m). As mentioned before, this safety factor is defined with respect to soil shear strength parameters $c$ and tan $\varphi$. For each curve, $F_s$ presents a maximum value

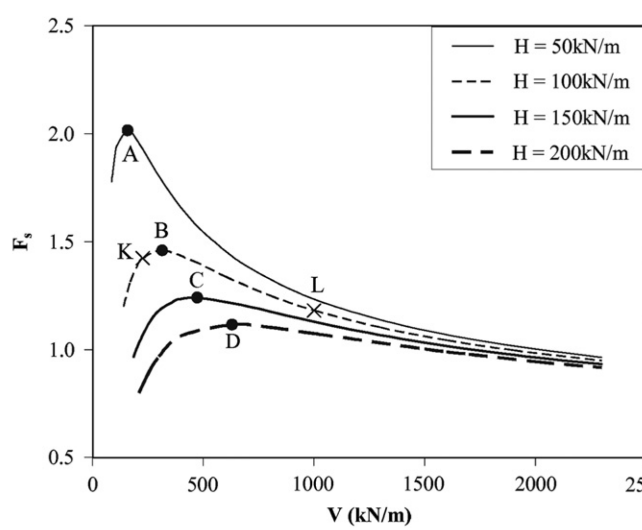


Fig. 3. Safety factor $F_s$ versus the vertical load component $V$ for different values of the horizontal load component $H$.

Table 2
Sobol indices for the different input random variables ($c$, $\varphi$, $V$, H) and the correlation coefficients between the input variables and the safety factor $F_s$.

| Input random variables | Sobol indices | | Correlation coefficient between ($c$, $\varphi$, $V$, $H$) and $F_s$ | |
|---|---|---|---|---|
| | Point K | Point L | Point K | Point L |
| $c$ | 0.110 | 0.178 | 0.39 | 0.42 |
| $\varphi$ | 0.127 | 0.702 | 0.42 | 0.84 |
| $V$ | 0.001 | 0.055 | 0.04 | −0.23 |
| $H$ | 0.745 | 0.062 | −0.80 | −0.24 |
| | Summation ≈ 1.00 | Summation ≈ 1.00 | | |

(see points A, B, C and D). The numerical results show that these maximum values for $F_s$ correspond exactly to the same ratio $H/V$, i.e., to the same load inclination $\alpha = 17.62^\circ$ represented by line OO′ in Fig. 2. This means that from a deterministic point of view, line OO′, that joins the origin and the maximum point of the interaction diagram, subdivides this diagram into two zones, one on the right-hand side of line OO′ (where the soil punching mode is predominant) and the other on the left-hand side of this line (where the footing sliding mode is predominant). This is due to the fact that for a given value of $H$, $F_s$ increases with an increase in $V$ in the zone of footing sliding predominance and it decreases with an increase in $V$ in the zone of soil punching predominance; its maximum value corresponds to the load configuration for which no failure mode is predominant. It should be mentioned here that the determination of the zones of predominance of punching or sliding described above is based on deterministic computations. It does not take into account the soil and/or the loading uncertainties. In order to check if the zones of sliding predominance and punching predominance are dependent on the load and/or the soil uncertainties, a probabilistic analysis is undertaken.

The failure probability is computed for different values of the vertical load component when the horizontal load component is equal to 100 kN/m (cf., Fig. 4) for the following three cases: (i) case ‘A’ where only loading components $V$ and $H$ are considered as random variables, (ii) case ‘B’ where only soil shear strength parameters $c$ and $\varphi$ are assumed to be random variables and (iii) case ‘C’ where $c$, $\varphi$, $V$ and $H$ are considered as random variables. Similar to case ‘C’, a fourth order *PCE* was found optimal for cases ‘A’ and ‘B’ (results not shown). Thus, the number of sampling points used in cases ‘A’ and ‘B’ (where the number of random variables is equal to 2) is equal to 15. Notice that the performance function used in the probabilistic calculation is $G = F_s - 1$, where $F_s$ is computed

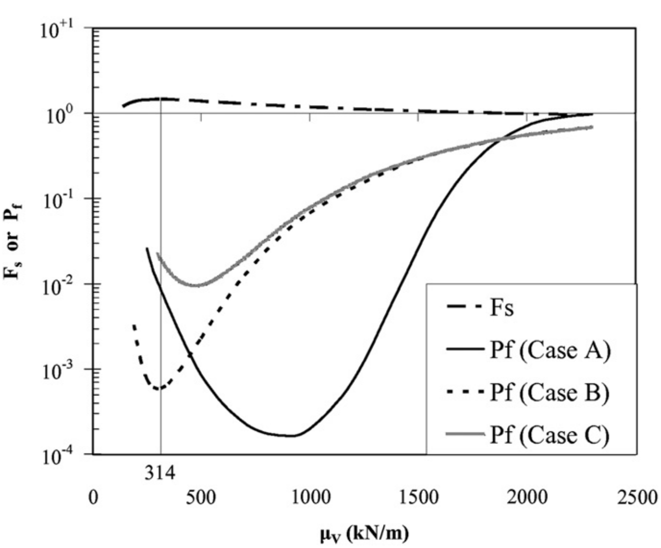


Fig. 4. Safety factor $F_s$ and failure probability $P_f$ versus $\mu_V$ when $\mu_H = 100$ kN/m.

using the strength reduction method. The failure probability (of each case of study) is determined using *MCS* by generating a large number (say $5 \times 10^6$) of realizations ($\xi_1, \xi_2, \xi_3, \xi_4$) and by computing the safety factor corresponding to each realization using the corresponding *PCE*. The failure probability is the ratio between the number of realizations for which $F_s < 1$ (i.e., $G < 0$) and the total number of realizations. It should be emphasized here that, since the safety factor simultaneously considers soil punching and footing sliding in a single simulation, the probabilistic analysis based on $G = F_s - 1$ takes into account both failure modes, and thus, directly provides the system failure probability and not the components' failure probabilities, $P_f$(punching) or $P_f$(sliding). This is the great advantage of the present approach using $F_s$ (based on the strength reduction technique), since one can avoid the approximation that arises from the application of the formula of the system failure probability (notice that the system failure probability is generally based on a simplified assumption concerning the dependence between both failure modes). Furthermore, only a unique probabilistic analysis was performed for both failure modes. Finally, it should be mentioned that another advantage of the safety factor used in this study is that it allows one to rigorously determine the zones of predominance of soil punching or footing sliding in the interaction diagram since the system failure probability is rigorously computed.

Failure probability $P_f$ is plotted against the mean value of vertical load component $\mu_V$ in Fig. 4 for the three above-mentioned cases. This figure also gives the safety factor versus deterministic vertical load component $V$ (or $\mu_V$ since $V = \mu_V$ for the deterministic analysis). For a given value of $\mu_H$, although the two modes of failure are present whatever the value of $\mu_V$ is, the footing sliding is predominant for small values of $\mu_V$. Thus, the failure probability of the system (sliding and punching) is mainly due to the footing sliding and this failure probability is significant. When vertical load component $\mu_V$ increases, the effect of footing sliding decreases and that of soil punching gradually increases until both modes of failure become non-predominant and induce a minimal value of the system failure probability. Beyond this value, an increase in vertical load component $\mu_V$ leads to an increase in the predominance of the punching mode with respect to the sliding one, and thus, to an increase in the failure probability of the system. It should be emphasized here that the term ‘sliding predominance’ means that the value of $P_f$ is mainly due to the footing sliding effect. Therefore, there is a high risk of failure against this mode of failure. This does not mean that there is no risk of failure against the punching mode of failure; however, the risk is smaller. The same explanation remains valid for the term ‘punching predominance’.

Fig. 4 shows that the minimum for $P_f$ and the maximum for $F_s$ correspond to the same values of the vertical load component only for case ‘B’ where the soil parameters are considered as random variables (the value of the vertical

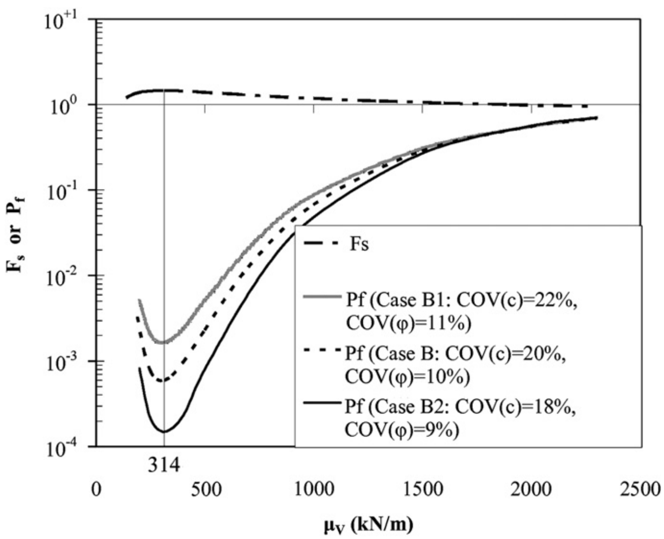


Fig. 5. $F_s$ or $P_f$ versus $V$ or $\mu_V$ for three different cases of soil uncertainties when $H$=100 kN/m.

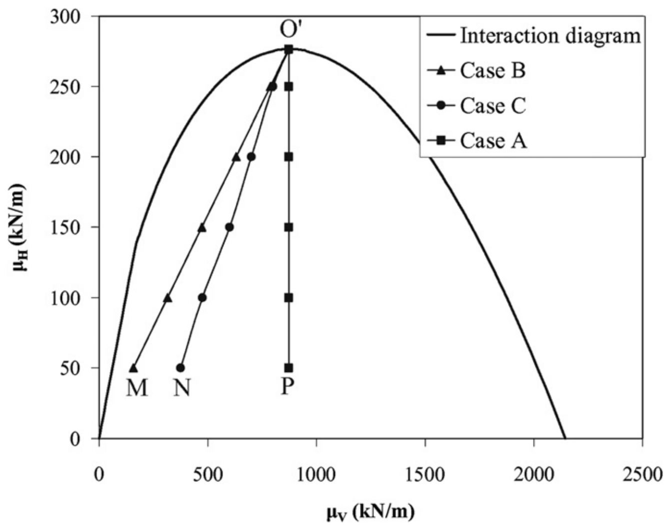


Fig. 6. Optimal load configurations corresponding to non-predominance of neither sliding nor punching for different cases of soil and/or load uncertainties.

load is $\mu_V$=314 kN/m, as may be seen in Fig. 4). This indicates that the probabilistic approach provides the same results as the deterministic approach in the case where only the uncertainties of the soil are considered. This may be explained by the fact that the optimal load inclination, leading to a maximal safety factor or a minimal failure probability, is not a function of the values of the soil uncertainties (see Fig. 5 where cases B1 and B2 correspond respectively to an increase and a decrease in the $COVs$ of $c$ and $\varphi$ by 10% with respect to the reference values given in Table 1). On the other hand, when only the uncertainties of the loading (i.e., case 'A') or the uncertainties of both the loading and the soil parameters (i.e., case 'C') are considered, the minimal value for $P_f$ corresponds to a greater value for $\mu_V$ ($\mu_V$=872 kN/m and $\mu_V$=475 kN/m for cases 'A' and 'C', respectively). Thus, the zone of footing sliding predominance in the interaction diagram extends with the presence of load uncertainties. This may be explained by the fact that horizontal load component $H$ has the most important contribution in the variability of $F_s$ in the zone of footing sliding predominance. Consequently, it would be expected that cases 'A' and 'C' (where $H$ is present) have a more extended sliding zone compared to case 'B' (which does not consider loading uncertainties).

One can conclude that, although the deterministic approach can provide the two zones of predominance, this possibility is limited to cases where only the uncertainties of the soil parameters are considered in the analysis. In such cases where the loading uncertainties are involved in the analysis, one cannot determine the two zones of predominance using a deterministic approach; a probabilistic analysis is necessary.

Finally, Fig. 6 presents the optimal load configurations in the interaction diagram corresponding to non-predominance of either sliding or punching and for which one obtains the minimal $P_f$ compared to other loading configurations having the same horizontal load component. These results are given for different cases of soil and/or loading uncertainties. They are obtained by repeating the computations made in Fig. 4 for different mean values of horizontal load component $\mu_H$. For case 'B', where only the soil uncertainties are considered, both the deterministic and the probabilistic approaches have found the same optimal load configurations corresponding to no sliding or punching predominance, as was the case for $\mu_H$=100 kN/m in Fig. 4. In this case (i.e., case 'B'), the zone of the footing sliding predominance (left-hand side of line O'M) is much smaller than that of the soil punching predominance. In the presence of both soil and loading uncertainties (i.e., case 'C'), this zone of footing sliding (left-hand side of line O'N) extends with respect to that of case 'B' and can be determined only by the probabilistic approach. Finally, in case 'A' where only the loading uncertainties are considered in the analysis, the sliding zone on the left-hand side of line O'P attains almost half of the interaction diagram. This means that the optimal load configurations corresponding to the non-predominance of either mode are situated on the vertical line passing through the maximum point of the interaction diagram. The fact that the optimal value of the vertical load component ($\mu_{Vopt}$) for a prescribed horizontal load component is that corresponding to the maximum point of the interaction diagram, may be explained by the following.

For values of vertical load component $\mu_V$ smaller or greater than $\mu_{Vopt}$, one obtains greater values of the failure probability due to either a sliding or a punching predominance. The greater values of the failure probability may be explained by the concept of dispersion ellipse (cf., Mollon et al., 2009, among others) as follows: For values of vertical load component $\mu_V$ smaller or greater than $\mu_{Vopt}$, one obtains smaller values for the Hasofer–Lind reliability index $\beta_{HL}$, as may be seen from Fig. 7 (i.e., greater values of the failure probability). Remember here that the

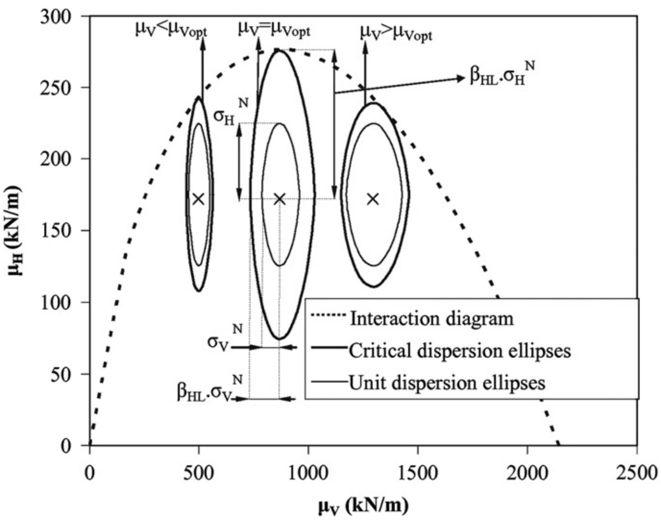


Fig. 7. Critical and unit dispersion ellipses for $\mu_H = 175$ kN/m and for three values of $\mu_V$ ($\mu_V < \mu_{V\text{opt}}$; $\mu_V = \mu_{V\text{opt}}$; $\mu_V > \mu_{V\text{opt}}$).

reliability index is the ratio between the critical dispersion ellipse that is tangent to the limit state surface (interaction diagram in the present case of loading uncertainties) and the unit dispersion ellipse. As may be easily seen from Fig. 7, this ratio is maximal at $\mu_{Vopt}$. Notice finally that in Fig. 7, $\sigma_V^N$ and $\sigma_H^N$ are the equivalent normal standard deviations of the vertical and horizontal load components respectively.

### 4.3. Variability of the system response and mode of failure predominance for some practical load configurations

This section aims at considering the effect of the footing load inclination on the *PDF* of the safety factor for the practical load configurations corresponding to $V_u/V = 3$ and $H_u/H = 3$ where $V_u$ and $H_u$ are, respectively, the ultimate vertical and horizontal load components corresponding to the load inclination considered in the analysis, while $V$ and $H$ are, respectively, the applied vertical and horizontal load components corresponding to the same load inclination. The case of non-normal and uncorrelated variables is considered in the analysis.

Fig. 8 presents the *PDF* of the safety factor for different load inclinations and for different cases of soil and/or load uncertainties (i.e., cases ‘A’, ‘B’ and ‘C’). The statistical moments corresponding to these *PDF*s are given in Table 3.

From Table 3, it can be easily seen that the variability of the safety factor obtained when considering both the soil and the loading uncertainties is smaller than the one obtained by the summation of the two variabilities computed separately. Thus, it is necessary to take into account all the input uncertainties of the soil and the loading in a single computation in order to obtain accurate results in cases where the soil and the loading uncertainties are present in the analysis.

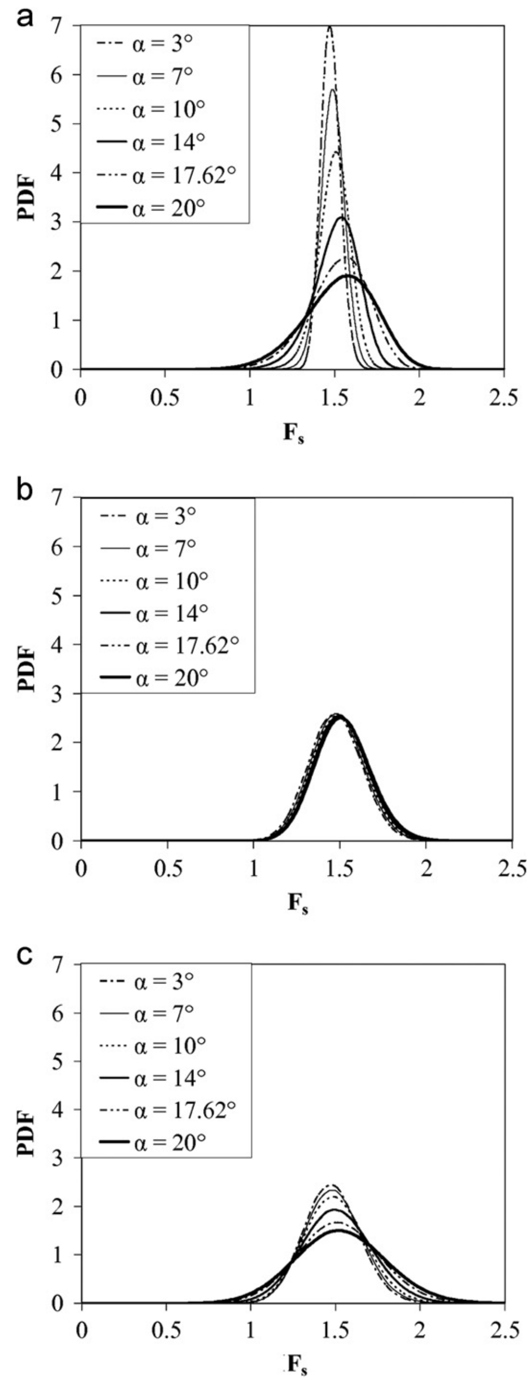


Fig. 8. *PDF* of $F_s$ for different load inclinations.

On the other hand, Table 3(b) and Fig. 8(b) show that the variability of $F_s$ does not significantly change with the increase in footing load inclination $\alpha$ when one considers only the soil uncertainties. This is due to the fact that for the different load inclinations considered in case ‘B’, (i) the safety factor is identical for the adopted values of $V$ and $H$, that respect $V_u/V = 3$ and $H_u/H = 3$, and (ii) the input variability (which is that of $c$ and $\varphi$) is similar regardless of the load inclination. Contrary to case ‘B’, for cases ‘A’ and ‘C’, the variability of the safety factor significantly increases with $\alpha$ (see Fig. 8(a) and (c) and Table 3(a) and

Table 3
Statistical moments ($\mu$,$\sigma$) of $F_s$ for different load inclinations.

| | **3°[a]** | **7°[a]** | **10°[a]** | **14°[a]** | **17.62°[a]** | **20°[a]** |
|---|---|---|---|---|---|---|
| (a) Case "A" with only load uncertainties | | | | | | |
| $\mu$ | 1.48 | 1.49 | 1.50 | 1.51 | 1.52 | 1.53 |
| $\sigma$ | 0.06 | 0.07 | 0.10 | 0.14 | 0.18 | 0.21 |
| **COV%** | 3.9 | 4.9 | 6.4 | 9.0 | 11.8 | 13.8 |
| | **3°[b]** | **7°[b]** | **10°[b]** | **14°[b]** | **17.62°[b]** | **20°[a]** |
| (b) Case "B" with only soil uncertainties | | | | | | |
| $\mu$ | 1.47 | 1.49 | 1.49 | 1.51 | 1.51 | 1.52 |
| $\sigma$ | 0.15 | 0.15 | 0.16 | 0.16 | 0.16 | 0.16 |
| **COV%** | 10.3 | 10.3 | 10.4 | 10.4 | 10.5 | 10.6 |
| | **3°[b]** | **7°[b]** | **10°[b]** | **14°[a]** | **17.62°[a]** | **20°[a]** |
| (c) Case "C" with both load and soil uncertainties | | | | | | |
| $\mu$ | 1.48 | 1.49 | 1.50 | 1.51 | 1.52 | 1.53 |
| $\sigma$ | 0.16 | 0.17 | 0.18 | 0.21 | 0.24 | 0.27 |
| **COV%** | 11.1 | 11.4 | 12.2 | 13.8 | 15.9 | 17.5 |

[a]Footing sliding predominance.
[b]Soil punching predominance.
[c]Non-predominance of neither footing sliding nor soil punching.

(c)), especially when $\alpha > 10°$. For instance, when $\alpha$ increases from 14° to 20°, the *COV* of $F_s$ increases by 52.7% in case 'A' compared to 26.1% in case 'C'. The significant increase in the variability of $F_s$ for $\alpha > 10°$ is to be expected, since the variability in the loading for great values of $\alpha$ induces much more variability in the safety factor due to the predominance of the footing sliding (where the variability of $H$ is of a significant effect). Finally, Table 3 shows that although case 'A' gives a footing sliding predominance for all the load inclinations considered in this table, case 'B' gives a footing sliding only for $\alpha > 17.62°$, while case 'C' gives a footing sliding for $\alpha \geq 14°$. This shows once again the importance of properly considering the soil and/or the load uncertainties in any reliability-based analysis in order to accurately determine the mode of failure predominance.

### 4.4. Parametric study

The aim of this section is to study the effect of the statistical characteristics of the input random variables (the coefficient of variation, the type of the probability density function and the correlation coefficient) on the *PDF* of the safety factor for both zones of punching or sliding predominance when the soil and footing load uncertainties are considered in the analysis.

#### 4.4.1. Effect of the coefficients of variation of the random variables

To investigate the impact of the *COV* of a certain random variable on the *PDF* of the safety factor, the *COV* of this random variable is increased or decreased by 50% with respect to its reference value given in Table 1 (except for *COV*($H$) which is increased or decreased by only 33.3% to remain in a reasonable range); however, the *COV*s of the other random variables are assumed to be constant (i.e., equal to their reference values).

Figs. 9 and 10 show the effect of the *COV* of the different random variables on the *PDF* of the safety factor for the two loading configurations (points K and L in Fig. 2) corresponding to a footing sliding or a soil punching predominance, respectively. To facilitate the comparison between the two figures, the same scale was used for the horizontal axes of these figures. The statistical moments corresponding to these *PDF*s are given in Tables 4 and 5, respectively.

The *PDF* of $F_s$ is more spread out in the zone of footing sliding predominance compared to that in the zone of soil punching predominance. This may be explained by the high variability of the horizontal load component (which is believed to be the most encountered value in practice) adopted in this paper. It should also be remembered that $H$ has the most significant weight in the variability of the safety factor. As expected, Figs. 9 and 10 show that an increase in the *COV* of one of the random variables leads to a more spread out *PDF*. Fig. 9 shows that the impact of the variability of $H$ is the most significant one (contrary to that of the variability of $V$ which is negligible) in the zone of sliding predominance. For instance, when increasing *COV*($H$) by 33.3% and *COV*($\varphi$) and *COV*($c$) by 50% of their reference values, Table 4 shows that the *COV* of the safety factor increases by 17.9%, 10.3% and 9.2%, respectively. On the other hand, the impact of the variability of $\varphi$ is the most significant one in the zone of punching predominance (Fig. 10). For instance, the *COV* of the safety factor increases respectively by 37.3% and 10.9% when increasing *COV*($\varphi$) and *COV*($c$) by 50% with respect to their reference values; however, it increases only by about 3% with the increase in *COV*($V$) and *COV*($H$). Notice that although the increase in *COV* of the different random variables increases the variability of the safety factor in both zones of predominance, it has practically no effect on the probabilistic mean value of this response (this value is shown to be slightly greater than the deterministic value calculated using the mean values of the input random variables (cf., Tables 4 and 5)). This means that the randomness of the input variables leads to a variability of the safety factor which is roughly centered on its deterministic value. From the above results, one can observe that the input parameters for which the *COV*s are of most significant influence on the variability of the safety factor are the same as those that have the largest contribution in the variability of this safety factor (as obtained using Sobol indices).

Finally, Tables 4 and 5 show the effect of the *COV* of the random variables on their Sobol indices SU. The increase/decrease in *COV* of one of the variables induces an increase/decrease in the Sobol index of this variable (i.e., in its "weight" in the variability of the safety factor), and it also induces a decrease/increase in the Sobol indices

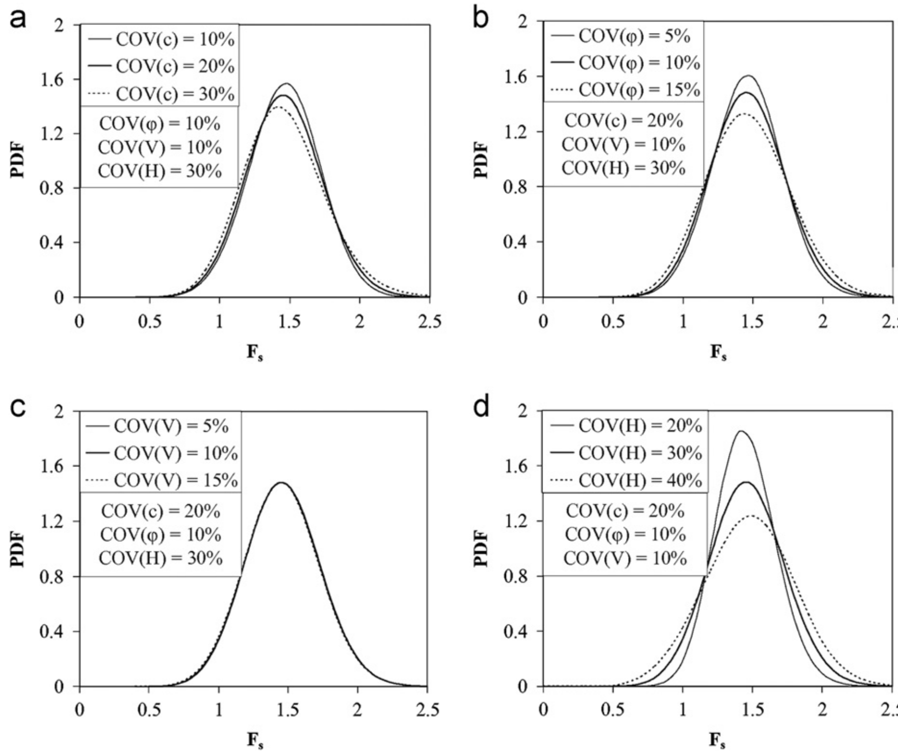


Fig. 9. Influence of the coefficients of variation of the input random variables on the *PDF* of the safety factor in the zone of footing sliding predominance. (a) Influence of COV(c), (b) Influence of COV(φ), (c) Influence of COV(V) and (d) Influence of COV(H).

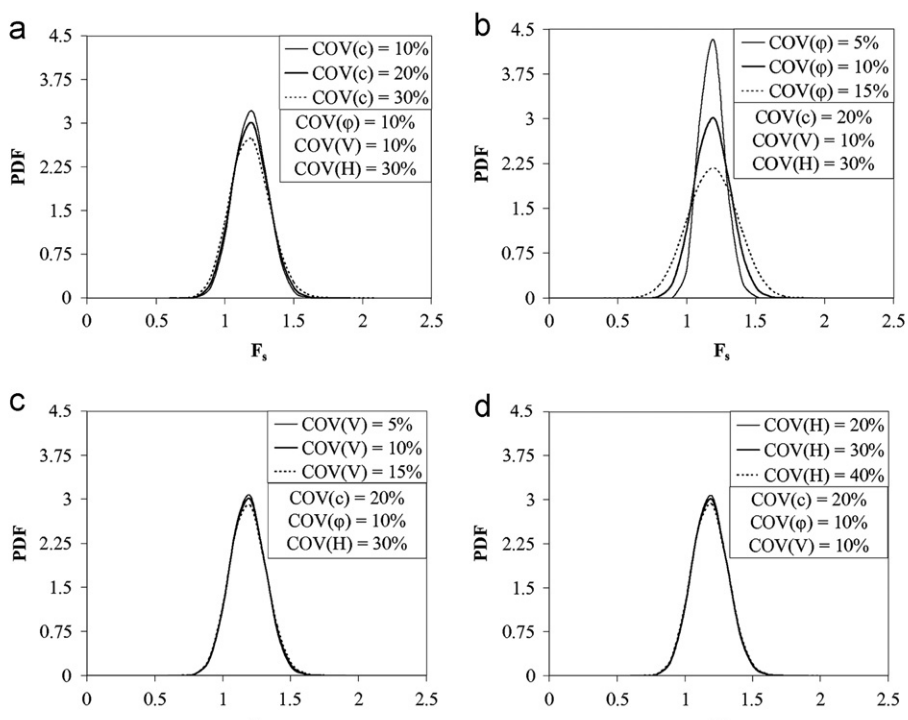


Fig. 10. Influence of the coefficients of variation of the input random variables on the *PDF* of the safety factor in the zone of soil punching predominance. (a) Influence of COV(c), (b) Influence of COV(φ), (c) Influence of COV(V) and (d) Influence of COV(H).

of the other variables. It should be emphasized here that the variation of the Sobol index is significant for the variables having the greatest weight in the variability of the safety factor (i.e., $H$ for the zone of footing sliding predominance and $\varphi$ for the zone of soil punching predominance).

Please cite this article as: Soubra, A.-H., Mao, N., Probabilistic analysis of obliquely loaded strip foundations. Soils and Foundations (2012), http://dx.doi.org/10.1016/j.sandf.2012.05.010

Table 4
Effect of the coefficients of variation of the input random variables on their Sobol indices SU and on the statistical moments ($\mu$, $\sigma$) of the safety factor in the zone of footing sliding predominance (i.e. point K).

| | $\mu$ | $\sigma$ | COV% | SU($c$) | SU($\varphi$) | SU($V$) | SU($H$) | Deterministic value of $F_s$ |
|---|---|---|---|---|---|---|---|---|
| COV($c$) | | | | | | | | |
| 10% | 1.46 | 0.25 | 17.3 | 0.043 | 0.201 | 0.002 | 0.741 | 1.45 |
| 20% | 1.46 | 0.27 | 18.4 | 0.152 | 0.177 | 0.002 | 0.654 | |
| 30% | 1.46 | 0.29 | 20.1 | 0.282 | 0.148 | 0.002 | 0.549 | |
| COV($\varphi$) | | | | | | | | |
| 5% | 1.46 | 0.25 | 17.1 | 0.176 | 0.051 | 0.002 | 0.756 | |
| 10% | 1.46 | 0.27 | 18.4 | 0.152 | 0.177 | 0.002 | 0.654 | |
| 15% | 1.47 | 0.30 | 20.3 | 0.123 | 0.325 | 0.002 | 0.535 | |
| COV($V$) | | | | | | | | |
| 5% | 1.47 | 0.27 | 18.3 | 0.154 | 0.180 | 0.000 | 0.656 | |
| 10% | 1.46 | 0.27 | 18.4 | 0.152 | 0.177 | 0.002 | 0.654 | |
| 15% | 1.46 | 0.27 | 18.6 | 0.148 | 0.173 | 0.006 | 0.650 | |
| COV($H$) | | | | | | | | |
| 20% | 1.45 | 0.22 | 14.9 | 0.230 | 0.270 | 0.005 | 0.484 | |
| 30% | 1.46 | 0.27 | 18.4 | 0.152 | 0.177 | 0.002 | 0.654 | |
| 40% | 1.48 | 0.32 | 21.7 | 0.110 | 0.127 | 0.001 | 0.745 | |

Table 5
Effect of the coefficients of variation of the input random variables on their Sobol indices SU and on the statistical moments ($\mu$, $\sigma$) of the safety factor in the zone of soil punching predominance (i.e. point L).

| | $\mu$ | $\sigma$ | COV% | SU($c$) | SU($\varphi$) | SU($V$) | SU($H$) | Deterministic value of $F_s$ |
|---|---|---|---|---|---|---|---|---|
| COV($c$) | | | | | | | | |
| 10% | 1.19 | 0.12 | 10.3 | 0.052 | 0.810 | 0.064 | 0.072 | 1.18 |
| 20% | 1.19 | 0.13 | 11.0 | 0.178 | 0.702 | 0.055 | 0.062 | |
| 30% | 1.18 | 0.14 | 12.2 | 0.324 | 0.576 | 0.045 | 0.051 | |
| COV($\varphi$) | | | | | | | | |
| 5% | 1.18 | 0.09 | 07.6 | 0.377 | 0.371 | 0.116 | 0.131 | |
| 10% | 1.19 | 0.13 | 11.0 | 0.178 | 0.702 | 0.055 | 0.062 | |
| 15% | 1.19 | 0.18 | 15.1 | 0.095 | 0.841 | 0.029 | 0.033 | |
| COV($V$) | | | | | | | | |
| 5% | 1.18 | 0.13 | 10.8 | 0.186 | 0.735 | 0.015 | 0.063 | |
| 10% | 1.19 | 0.13 | 11.0 | 0.178 | 0.702 | 0.055 | 0.062 | |
| 15% | 1.19 | 0.14 | 11.4 | 0.168 | 0.653 | 0.114 | 0.061 | |
| COV($H$) | | | | | | | | |
| 20% | 1.19 | 0.13 | 10.8 | 0.185 | 0.728 | 0.057 | 0.029 | |
| 30% | 1.19 | 0.13 | 11.0 | 0.178 | 0.702 | 0.055 | 0.062 | |
| 40% | 1.19 | 0.13 | 11.3 | 0.170 | 0.669 | 0.053 | 0.104 | |

#### 4.4.2. *Effect of the non-normality of the random variables and the correlation coefficient between variables*

For both zones of punching or sliding predominance, (i.e., for points K and L of Fig. 2), Fig. 11 presents the *PDF* of the safety factor for normal and non-normal variables. Two configurations of *COV*s were considered. The “Standard COVs” correspond to the reference values of the *COV* presented in Table 1, while the “High COVs” correspond to cases where $COV(c)=30\%$, $COV(\varphi)=15\%$, $COV(V)=15\%$ and $COV(H)=30\%$. For these two sets of *COVs*, the non-normality has a small influence on the *PDF* of the safety factor in the zone of footing sliding predominance (Fig. 11(a)), while there is almost no effect in the zone of soil punching predominance (Fig. 11(b)).

On the other hand, some authors [Harr (1987) and Cherubini (2000) among others] have suggested a negative correlation between effective cohesion $c$ and effective angle of internal friction $\varphi$. However, further experimental tests

Please cite this article as: Soubra, A.-H., Mao, N., Probabilistic analysis of obliquely loaded strip foundations. Soils and Foundations (2012), http://dx.doi.org/10.1016/j.sandf.2012.05.010

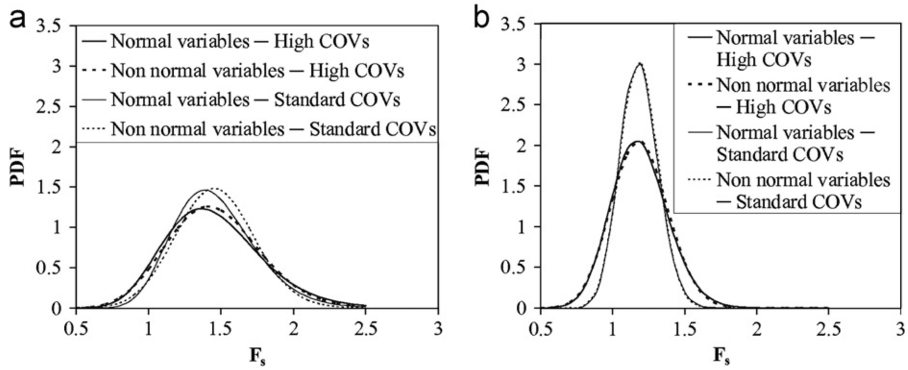


Fig. 11. Influence of the non-normality of the input random variables on the *PDF* of safety factor for two sets of the coefficients of variation of the random variables.

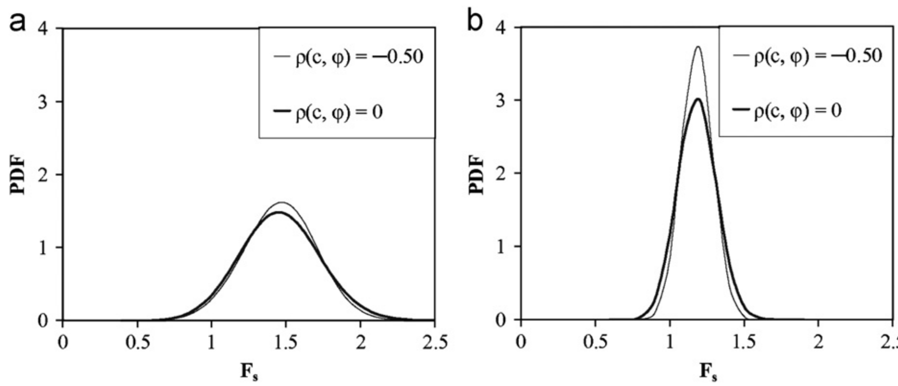


Fig. 12. Influence of the correlation coefficient $\rho(c, \varphi)$ on the *PDF* of safety factor. (a) Zone of footing sliding predominance and (b) Zone of soil punching predominance.

are needed to confirm this statement. Fig. 12 presents the effect of $\rho(c, \varphi)$ on the *PDF* of the safety factor for the two loading configurations represented by points K and L in Fig. 2. It appears that for both zones of sliding or punching predominance, the increase in $\rho(c, \varphi)$ increases the variability of $F_s$. For instance, the increase in $\rho(c, \varphi)$ from $-0.5$ to 0 increases the variability of the safety factor by 9.5% in the zone of footing sliding predominance and by 24.1% in the zone of soil punching predominance. One can conclude that assuming uncorrelated shear strength parameters is conservative in comparison to assuming negatively correlated parameters.

## 5. Conclusion

A probabilistic analysis of an obliquely loaded strip footing resting on a ($c$, $\varphi$) soil has been performed. The deterministic model was based on the kinematical approach of the limit analysis theory. The Polynomial Chaos Expansion (*PCE*) methodology was used for the probabilistic analysis. The input random variables considered in the analysis were the soil shear strength parameters ($c$ and $\varphi$) and the applied load components ($V$ and $H$). The general conclusions of the paper can be summarized as follows:

- The use of safety factor $F_s$, determined with the strength reduction method, allows one to rigorously compute the failure probability for a given load configuration ($V$ and $H$) since one does not need to perform a system reliability computation based on the values of the reliability of both components (footing sliding and soil punching).
- Although the deterministic approach can provide the zone of footing sliding predominance and that of soil punching predominance in the interaction diagram, this possibility is limited to cases where only the soil uncertainties are considered. In cases where the load uncertainties are involved in the analysis, one cannot determine the two zones of predominance using a deterministic approach; a probabilistic analysis is necessary. In the interaction diagram, the zone of footing sliding predominance is much smaller than that of the soil punching predominance when only the soil uncertainties are considered in the analysis. This zone extends to almost half of the interaction diagram when one considers only the loading uncertainties in the analysis.

Please cite this article as: Soubra, A.-H., Mao, N., Probabilistic analysis of obliquely loaded strip foundations. Soils and Foundations (2012), http://dx.doi.org/10.1016/j.sandf.2012.05.010

– The global sensitivity analysis, using the Sobol indices, has shown that for the adopted values of the statistical parameters of the random variables (which are believed to be frequently encountered in practice), the horizontal load component and the soil friction angle have a significant weight in the variability of the safety factor in the zones of footing sliding and soil punching predominance, respectively.
– It was observed that a high correlation exists between an input random variable and safety factor $F_s$ when the Sobol index of this variable is significant.
– In both zones of sliding or punching predominance, the probabilistic mean value of the safety factor remains almost the same with the increase in $COV$ of the different random variables. It is close to the deterministic value computed using the mean values of the random variables. This means that the randomness of the input variables leads to a variability of the safety factor which is roughly centered on its deterministic value. On the other hand, the variability of the safety factor increases with the increase in $COV$ of the random variables (as expected) and it is more sensitive to the variation of $COV(H)$ in the zone of footing sliding predominance and to the variation of $COV(\varphi)$ in the zone of soil punching predominance.
– The variability of $F_s$ was found to be more significant in the zone of sliding predominance.
– It was observed that the input parameters, for which the $COV$s are of most significant influence on the variability of the safety factor, are the same as those that have the largest contribution in the variability of this safety factor (as obtained using Sobol indices).
– The increase/decrease in $COV$ of one of the random variables induces an increase/decrease in the Sobol index of this variable (i.e., in its "weight" in the variability of the safety factor), and it also induces a decrease/increase in the Sobol indices of the others variables. The variation of the Sobol index is significant for the variables having the greatest weight in the variability of the safety factor (i.e., $H$ for the zone of footing sliding predominance and $\varphi$ for the zone of soil punching predominance).
– The non-normality of the probability density function of the input random variables has practically no effect on the $PDF$ of $F_s$.
– In both zones of punching or sliding predominance, the increase in the correlation coefficient between $c$ and $\varphi$ in the interval $[-0.5, 0]$ increases the variability of $F_s$. Consequently, assuming uncorrelated shear strength parameters (when rigorous information about correlation is absent) is conservative in comparison to assuming negatively correlated variables.
– For the practical load configurations, the variability of $F_s$ does not change with the increase in the footing load inclination when one considers only the soil uncertainties. However, this variability significantly increases with $\alpha$, especially when $\alpha > 10°$, if one considers either the load uncertainties or both the load and the soil uncertainties. Also, the mode of failure predominance was shown to be closely related to the uncertainties considered in the analysis (i.e., those of the soil and/or the loading).

## Appendix. Multidimensional Hermite polynomial

The multidimensional Hermite polynomial is the product of the one-dimensional Hermite polynomials for the different random variables.

Within the framework of the Polynomial Chaos Expansion methodology (see Eq. (3)), only the multidimensional Hermite polynomials of a degree smaller than or equal to $p$ are retained to construct the $PCE$ of order $p$. As an example, Table A1 shows the multidimensional Hermite polynomials of a degree smaller than or equal to 4 in the case of 2 random variables. These polynomials are used to construct the $PCE$ of order $p=4$ with $M=2$ random variables. In this case, the number of the $PCE$ coefficients $a_\beta$ is $P=((p+M)!/p!M!)=((2+4)!/2!4!)=15$. The construction of other $PCE$s corresponding to other values of $p$ and $M$ is straightforward.

Table A1
Multidimensional Hermite polynomial of degree smaller than or equal to 4 in the case of 2 random variables.

| $\beta$ | Coefficients, $a_\beta$ | Degree, $p$ | Multidimensional Hermitepolynomials $\Psi_\beta$ |
|---|---|---|---|
| 0 | $a_0$ | 0 | $H^{(0)}(\xi_1)*H^{(0)}(\xi_2)=1$ |
| 1 | $a_1$ | 1 | $H^{(1)}(\xi_1)*H^{(0)}(\xi_2)=\xi_1$ |
| 2 | $a_2$ | 1 | $H^{(0)}(\xi_1)*H^{(1)}(\xi_2)=\xi_2$ |
| 3 | $a_3$ | 2 | $H^{(2)}(\xi_1)*H^{(0)}(\xi_2)=\xi_1^2-1$ |
| 4 | $a_4$ | 2 | $H^{(1)}(\xi_1)*H^{(1)}(\xi_2)=\xi_1\xi_2$ |
| 5 | $a_5$ | 2 | $H^{(0)}(\xi_1)*H^{(2)}(\xi_2)=\xi_2^2-1$ |
| 6 | $a_6$ | 3 | $H^{(3)}(\xi_1)*H^{(0)}(\xi_2)=\xi_1^3-3\xi_1$ |
| 7 | $a_7$ | 3 | $H^{(2)}(\xi_1)*H^{(1)}(\xi_2)=\xi_1^2\xi_2-\xi_2$ |
| 8 | $a_8$ | 3 | $H^{(1)}(\xi_1)*H^{(2)}(\xi_2)=\xi_1\xi_2^2-\xi_1$ |
| 9 | $a_9$ | 3 | $H^{(0)}(\xi_1)*H^{(3)}(\xi_2)=\xi_2^3-3\xi_2$ |
| 10 | $a_{10}$ | 4 | $H^{(4)}(\xi_1)*H^{(0)}(\xi_2)=\xi_1^4-6\xi_1^2+3$ |
| 11 | $a_{11}$ | 4 | $H^{(3)}(\xi_1)*H^{(1)}(\xi_2)=\xi_1^3\xi_2-3\xi_1\xi_2$ |
| 12 | $a_{12}$ | 4 | $H^{(2)}(\xi_1)*H^{(2)}(\xi_2)=\xi_1^2\xi_2^2-\xi_1^2-\xi_2^2+1$ |
| 13 | $a_{13}$ | 4 | $H^{(1)}(\xi_1)*H^{(3)}(\xi_2)=\xi_1\xi_2^3-3\xi_1\xi_2$ |
| 14 | $a_{14}$ | 4 | $H^{(0)}(\xi_1)*H^{(4)}(\xi_2)=\xi_2^4-6\xi_2^2+3$ |

Please cite this article as: Soubra, A.-H., Mao, N., Probabilistic analysis of obliquely loaded strip foundations. Soils and Foundations (2012), http://dx.doi.org/10.1016/j.sandf.2012.05.010

## References

Bauer, J., Pula, W., 2000. Reliability with respect to settlement limit-states of shallow foundations on linearly-deformable subsoil. Computers and Geotechnics 26, 281–308.

Berveiller, M., Sudret, B., Lemaire, M., 2006. Stochastic finite elements: a non intrusive approach by regression. European Journal of Computational Mechanics 15 (1–3), 81–92.

Cherubini, C., 2000. Reliability evaluation of shallow foundation bearing capacity on $C'$, $\varphi'$ soils. Canadian Geotechnical Journal 37, 264–269.

De Buhan, P., Garnier, D., 1998. Three dimensional bearing capacity analysis of a foundation near a slope. Soils and Foundations 38 (3), 153–163.

Fenton, G.A., Griffiths, D.V., 2002. Probabilistic foundation settlement on spatially random soil. Journal of Geotechnical and Geoenvironmental Engineering, ASCE 128 (5), 381–390.

Fenton, G.A., Griffiths, D.V., 2003. Bearing capacity prediction of spatially random $c$–$\varphi$ soils. Canadian Geotechnical Journal 40, 54–65.

Griffiths, D.V., Fenton, G.A., 2001. Bearing capacity of spatially random soil: the undrained clay Prandtl problem revisited. Géotechnique 51 (4), 351–359.

Griffiths, D.V., Fenton, G.A., Manoharan, N., 2002. Bearing capacity of rough rigid strip footing on cohesive soil: probabilistic study. Journal of Geotechnical and Geoenvironmental Engineering, ASCE 128 (9), 743–755.

Harr, M.E., 1987. Reliability-based Design in Civil Engineering. McGraw-Hill Book Company, New York 290 pp.

Houmadi, Y., Ahmed, A., Soubra, A.-H., 2012. Probabilistic analysis of a one-dimensional soil consolidation problem. Georisk: Assessment and Management of Risk for Engineered Systems and Geohazards 6 (1), 36–49.

Huang, S.P., Liang, B., Phoon, K.K., 2009. Geotechnical probabilistic analysis by collocation-based stochastic response surface method: an EXCEL Add-in implementation. Georisk: Assessment and Management of Risk for Engineered Systems and Geohazards 3 (2), 75–86.

Huang, J., Griffiths, D.V., Fenton, G.A., 2010. System reliability of slopes by RFEM. Soils and Foundations 50 (3), 343–353.

Isukapalli, S.S., Roy, A., Georgopoulos, P.G., 1998. Stochastic response surface methods (SRSMs) for uncertainty propagation: application to environmental and biological systems. Risk Analysis 18 (3), 357–363.

Kusakabe, O., Kimura, T., Yamaguchi, H., 1981. Bearing capacity of slopes under strip loads on the top surfaces. Soils and Foundations 21 (4), 29–40.

Kusakabe, O., Kobayashi, S.-I., 2010. Foundations. Soils and Foundations 50 (6), 903–913.

Mao, N., Al-Bittar, T., Soubra, A.-H., 2012. Probabilistic analysis and design of strip foundations resting on rocks obeying Hoek–Brown failure criterion. International Journal of Rock Mechanics and Mining Sciences 49 (1), 45–58.

Michalowski, R.L., 1997. An estimate of the influence of soil weight on bearing capacity using limit analysis. Soils and Foundations 34 (7), 57–64.

Mollon, G., Dias, D., Soubra, A.H., 2009. Probabilistic analysis and design of circular tunnels against face stability. International Journal of Geomechanics, ASCE 9 (6), 237–249.

Mollon, G., Dias, D., Soubra, A.H., 2011. Probabilistic analysis of pressurized tunnels against face stability using collocation-based stochastic response surface method. Journal of Geotechnical and Geoenvironmental Engineering, ASCE 137 (4), 385–397.

Phoon, K.K., Kulhawy, F.H., 1999. Evaluation of geotechnical property variability. Canadian Geotechnical Journal 36, 625–639.

Popescu, R., Deodatis, G., Nobahar, A., 2005. Effects of random heterogeneity of soil properties on bearing capacity. Probabilistic Engineering Mechanics 20, 324–341.

Przewlocki, J., 2005. A stochastic approach to the problem of bearing capacity by the method of characteristics. Computers and Geotechnics 32, 370–376.

Sivakumar Babu, G.L., Srivastava, A., 2007. Reliability analysis of the allowable pressure on shallow foundation using response surface method. Computers and Geotechnics 34, 187–194.

Soubra, A.H., 1999. Upper-bound solutions for bearing capacity of foundations. Journal of Geotechnical and Geoenvironmental Engineering, ASCE 125 (1), 59–68.

Sudret, B., 2008. Global sensitivity analysis using polynomial chaos expansion. Reliability Engineering and System Safety 93, 964–979.

Youssef Abdel Massih, D.S., Soubra, A.-H., Low, B.K., 2008. Reliability-based analysis and design of strip footings against bearing capacity failure. Journal of Geotechnical and Geoenvironmental Engineering, ASCE 134 (7), 917–928.

Youssef Abdel Massih, D.S., Soubra, A.-H., 2008. Reliability-based analysis of strip footings using response surface methodology. International Journal of Geomechanics, ASCE 8 (2), 134–143.

Please cite this article as: Soubra, A.-H., Mao, N., Probabilistic analysis of obliquely loaded strip foundations. Soils and Foundations (2012), http://dx.doi.org/10.1016/j.sandf.2012.05.010